*Turk. J. Fish.& Aquat. Sci. 24(5), TRJFAS24434*
https://doi.org/10.4194/TRJFAS24434

PROOF
RESEARCH PAPER

Turkish Journal of FISHERIES and AQUATIC SCIENCES

# Simultaneous Removal of Toxic Ammonia ($NH_3/NH_4^+$) from Aqueous Solutions Using New Geomaterial Adsorbent: Application to Aquaculture Effluents

**Nassima Belhouchet*[,1], Boualem Hamdi[2,3], Omar Bouras[4]**

[1]Centre National de Recherche et de Développement de la Pêche et d'Aquaculture, Tipaza, Algérie.
[2]Ecole Nationale Supérieure des Sciences de la Mer et de l'Aménagement du Littoral, Algiers, Algérie.
[3]Laboratoire d'Etude Physico-Chimique des Matériaux et Application à l'Environnement, Faculté de chimie, Université des Sciences et de la Technologie Houari Boumediene, Alger, Algérie.
[4]Laboratoire Eau Environnement et Développement Durable, Faculté de Technologie, Université de Blida 1, Blida, Algérie.

**How to Cite**

Belhouchet, N., Hamdi, B., Bouras, O. (2024). Simultaneous Removal of Toxic Ammonia ($NH_3/NH_4^+$) from Aqueous Solutions Using New Geomaterial Adsorbent: Application to Aquaculture Effluents. *Turkish Journal of Fisheries and Aquatic Sciences*, *24(5), TRJFAS24434.* https://doi.org/10.4194/TRJFAS24434

**Article History**
Received 03 August 2023
Accepted 01 March 2024
First Online 13 March 2024

**Corresponding Author**
E-mail: belhouchet.n@gmail.com

**Keywords**
Recirculating Aquaculture System
Ammonium ($NH_4^+/NH_3$)
Geomaterial
Adsorption
Biofilter

## Abstract

This study evaluates the performance of a new geomaterial (GEOM) based on sodium montmorillonite clay (Na-Mt), local activated carbon (CAC) and fine powder local cement (Chlef plant western Algeria) to remove ammonia from fish farming in a recirculating aquaculture system. The aqueous ammonium ($NH_4^+/NH_3$) adsorption efficiency of GEOM was compared with its two principals' constituents (Na-Mt and CAC) and another commercial activated carbon (CAG). The results of X-ray diffraction (XRD) and Fourier transform infrared (FTIR) spectroscopy were used to assess the chemical and physicochemical properties of studied adsorbents. The maximum adsorption capacity of $NH_4^+$ on GEOM of about 15.57 mg. $g^{-1}$ seems to be similar to that of Na-Mt 16.82 mg. $g^{-1}$. The study of solution pH showed that the best $NH_4^+/NH_3$ removal efficiency was at pH=6 for both GEOM and Na-Mt. The efficiency of GEOM for ammoniacal nitrogen ($NH_4^+/NH_3$) removal was 79.3% in ultrapure water, 94.05% in seawater and 97.5% in real aquaculture wastewater**.** Thus, the proposed material, GEOM, can be used as a filter material in a bio-filtration process to treat aquaculture wastewater in a real-world context.

## Introduction

The development of aquaculture technology allows users to reduce their dependence on captured fisheries and remedy the phenomenon of the observed decline in the number of fish (Boyd et al., 2020; Gephart et al., 2020). Indeed, the global growth of aquaculture industries has led to a diversification of undesirable environmental impacts through the discharge of substantial amounts of polluting effluents containing uneaten feed and feces (Chávez-Crooker and Obreque-Contreras, 2010; Ahmad et al., 2022). Also, the intensive development in the aquaculture industry has caused major environmental impacts (Mook et al., 2012). These various aquaculture wastewater discharges contain many nitrogenous compounds (ammonia, nitrite, and nitrate), phosphorus, and organic matter resulting from food remains and fish excrement (Dauda et al., 2019; Mavraganis et al., 2020). It causes environmental deterioration and local impacts at high concentrations, such as eutrophication and algal blooms (Nora'aini et al., 2005; Dauda et al., 2019).

In aquaculture, ammonia is the predominant form of nitrogenous wastewater (John, Krishnapriya, and Sankar, 2020; Liu et al., 2023) Ammonium exists in water either as ammonium ions or as non-ionized ammonia ($NH_3$) (Peterson, Bahr, and Kling, 1997; Radu and Racoviteanu, 2021). They are used to describe nutrient availability and nitrogen dynamics in water (Belhouchet et al., 2024). Total ammonia nitrogen is referred to as

the sum of $N\text{-}NH_4^+$ and $N\text{-}NH_3$ (Wang, Li, Chen, et al., 2020). The relative proportions of $NH_3$ and $NH_4^+$ depend on pH, temperature, and, to a lesser extent, salinity (Dunegan, 2020). The $NH_3$form is bioavailable and toxic to most aquatic animals due to its ability to diffuse through gill membranes (Cheng et al., 2019). At concentrations above 40µg. $L^{-1}$, ammonia species ($NH_3$) can cause respiratory stress to fish and make them more vulnerable to parasitic and infectious agents (Haywood, 1983; Person-Le Ruyet and Bœuf, 1998; Ip, Chew, and Randall, 2001). The assimilation of the nitrogen oxyanions as nutrients by aquatic plants, i.e., algae and phytoplankton, leads to eutrophication and perturbs the eco- stability (Mook et al., 2012; Belhouchet et al., 2024). Growing awareness of the harmful effects of ammonia discharged from wastewater treatment facilities into natural water systems has resulted in the adoption of laws and regulations limiting the discharge of ammonia (Bernet et al., 2000; Değermenci and Yildiz, 2021).

Consequently, many attempts have been made to remove ammonia from water systems. The approaches include biological treatment, chemical precipitation, flocculation and coagulation, adsorption, and ion exchange processes (Değermenci and Yildiz, 2021). Biofiltration is a traditional technology widely used to remove ammonia $N\text{-}NH_4^+$ in aquaculture wastewater, mainly including physical, chemical, biological, and integrated treatment processes (Liu et al., 2020). Biofiltration is one of the traditional technology widely in aquaculture to remove aqueous ammonium wastewater, mainly including physical, chemical, biological, and integrated treatment processes (Liu et al., 2020). It consists of a large compartment filled with materials comprising specific grooves for a maximum surface area where bacteria can be established in biofilms (Roalkvam et al., 2020). The advantage of biofilters is applying micro-organisms to remove these nitrogenous wastes from fish feces and residual feeds (Jiang et al., 2019). Ammonia and nitrite are removed through nitrification, first by oxidizing ammonium into nitrite and then further oxidizing nitrite into nitrate (Schreier, Mirzoyan, and Saito, 2010; Preena, Rejish Kumar, and Singh, 2021; Tuyet et al., 2022; Su et al., 2023). This reaction is achieved by autotrophic bacteria, such as ammonia-oxidizing bacteria and nitrite-oxidizing bacteria (Ruiz et al., 2020). Therefore, a healthy and stable microbial community can efficiently perform waste removal (Jiang et al., 2019). To optimize the removal of waste compounds, the biofilter should receive a stable supply of ammonia and organic matter (Blancheton et al., 2013). However, the biological method may be ineffective in treating saline water (Lee et al., 2019; Roalkvam et al., 2020). Furthermore, the water to be purified must have a pH adapted for the purifying bacteria and be free of any chemicals likely to harm the biological performance of the bacteria, such as chlorine and antibiotics, which presents an additional burden for the aquaculturist. In addition, there are other disadvantages linked mainly to the poor elimination of excess biofilms, the high consumption of dissolved oxygen, the high production of $CO_2$, the biofouling of sandy environments, the high pumping costs, the speed of anoxia of sand beds which would lead to pressure losses, particularly in mechanical and/or biological filtration (Hammer, 2020).

In another way, innovations in biofiltration can provide effective solutions to overcome crucial water pollution problems (Suprihatin et al., 2017). Adsorption to solid media has many favorable characteristics, including high removal efficiency, ease of operation, and low energy consumption. These significant advantages make it a promising method to be applied on a commercial scale (Cruz et al., 2019). As a result, numerous adsorbent materials have been studied due to the impact of $NH_3/NH_4^+$ emissions.

In this research area, natural and/or modified materials based on clays (Na-Mt, etc.), zeolite, and biochar were used to remove $NH_4^+$ in aqueous phases, while activated carbon and metal organic frameworks MOFs were employed to eliminate $NH_3$ in gas phases (DeCoste and Peterson, 2014; Xu et al., 2022). Even though conventional materials are relatively abundant and low-cost, their affinities towards $NH_3/NH_4^+$ have been shown to be low (Han et al., 2021). The adsorption process has been extensively used in recirculating aquaculture systems to remove organic chemicals and total organic carbon TOC (Rosenthal 1993). The most important parameters in this method are porosity and BET-specific surface area (Mook et al., 2012). However, those materials were only prepared in the laboratory with tedious preparation procedures using expensive precursors. Hence, the yield is low, and material properties vary greatly (Han et al., 2021).

This study proposes a new geocomposite adsorbent called GEOM. This material is made by mixing sodium montmorillonite (Na-Mt) activated carbon and fine powder cement. These three local constituents, which are economically less expensive than commercial substrates, will be able to eliminate important nitrogenous and carbonaceous pollutants from aquaculture discharges.

Practically, sorption tests are carried out to examine and evaluate the treatment performance of aquaculture waste in the elimination of ammonia pollution in aqueous medium.

The advantages of using this type of material include high adsorption capacity, low production costs, environmentally friendly consequences, unchanged molecular structure in the separation process at room temperature, and no product accumulation in the membrane.

This study, therefore, proposes the following steps: (i) Development and use of a new elaborate adsorbent GEOM based on (Montmorillonite) Na-Mt constituent as natural aluminosilicate, natural activated carbon CAC, and PC fine powders of cement (These three local constituents, which are economically less expensive

than commercial substrates, will be able to eliminate important nitrogenous and carbonaceous pollutants from aquaculture discharges); (ii): Sorption tests onto GEOM of ammonia existing at high concentrations in aquaculture discharges; (iii): Selection of the most promising sorbents for a possible more detailed study of their behavior in an adsorption process in both discontinuous and continuous systems for aquaculture wastewater.

## Material and Methods

### Reagents

All reagents were of analytical grade and used without further purification, and deionized water was used throughout the experiments. The ammonia stock solution is prepared by dissolving 1g.$L^{-1}$ of ammonium chloride $NH_4Cl$ stock solution with deionized water. This solution was used for successive dilutions to prepare synthetic solutions used in the other tests. Ammonium concentration was measured by an automatic method using "Auto-Analyzer SAN PLUS" based on continuous flow colorimetry. The operation of the device is based on a simple dynamic principle, that of liquid analysis in continuous flow: the determination of ammonium ($NH_4^+$) is carried out according to the method of Koroleff (1969) (Aminot and Chaussepied 1983).

### Sorbents

#### *Montmorillonite Homoionization*

Montmorillonite (Mt) furnished by ENOF Company (Maghnia deposit from western Algeria) was used as a starting material. It is composed essentially of montmorillonite (Mt) (75%) with minor impurities (quartz, feldspar, calcite) and was described previously in several works. To obtain the sodic-montmorillonite (Na-Mt), the raw Mt sample was immersed into NaCl (1 M) solution. Montmorillonite homoionization was carried out according to the protocol cited by (Khalaf et al., 1997; Melouki et al., 2022). The recovered powder is sodic-montmorillonite (Na-Mt). All these experiments were accomplished at room temperature (T=25±01°C) (Melouki et al., 2022).

#### *Geomaterial Preparation*

The new geomaterial GEOM was prepared by mixing (70%) purified homoionized montmorillonite (Na-Mt) with (5%) of activated carbon (CAC) (olive kernels-based), 10% of fine powder cement (Chlef plant in western Algeria containing 94.8% w/w $SiO_2$), and finally, a fine amount of polymer and silica. The organic phase is a water-soluble polymer. The preparation of this geomaterial GEOM is illustrated previously by (Hamdi et al., 2004; Houari et al., 2014). The mixtures of all constituents were kept for 72 h under moderate agitation (160 rpm). Obtained geomaterial is outside dried for several days and then stored at ambient temperature (T=20±1°C) (Figure 1).

#### *Adsorbent Characterization*

Prepared adsorbents were characterized by several experimental techniques such as chemical composition analysis using an XRF spectrometer PW2400 model, SEM (environmental scanning electron microscope) using Philips XL30 FEG for surface images at

**Figure 1.** Digital photo of the elaborate geocomposite GEOM

nanometric scales, Fourier Transform Infrared (FTIR) using (Nicolet Magna-IR 760 Fourier transform spectrometer equipped with KBr separator). Specific surface area and pore volume have been determined using a volumetric device of type Micromeritics Asap2010. XRD characterization was carried out by using a Panalytical diffractometer X'pertPro MPD theta / 2theta (Philips).

**Batch Adsorption Experiments**

Batch experiments were performed to examine the effects of pH, temperature and initial $NH_4^+$ concentration, on ammonium adsorption on Na-Mt, GEOM, CAC and CAG matrices. These experiments were realized at room temperature (20±1°C). All batch adsorption experiments were carried out using Erlenmeyer (100 mL) in a thermostatic shaker with a solid/liquid ratio of 50 mg/50 ml.

***Adsorption Kinetic Experiments***

The optimum time required for the $NH_4^+$ adsorption to attain equilibrium was determined as a function of contact time in the range of 0 to120 min of 20 mg $L^{-1}$ $NH_4^+$ solutions at a fixed pH of 7 and 20°C.

***Effect of the pH***

The pH effect was tested in the system (Concentration: 20 mg $NH_4^+$/L; Contact time; 2 h; pH range of 3 to 10). Accomplished kinetic studies determined this contact time at 20°C for the four substrates. The initial pH was adjusted by adding a few drops of 1 M (HCl or NaOH) solutions.

***Effect of the Temperature***

The influence of temperature on the retention of ammonia was also studied by working at several temperatures (10, 20, and 30°C). The volume was fixed at 50 mL of $NH_4Cl$ solution but in several different concentrations (2 to 50 mg. $L^{-1}$).

***Adsorption Isotherms***

The effect of the initial concentration of ammonia on the capacity for the elimination of $NH_4^+$ was evaluated by bringing into contact in several identical Erlenmeyer flasks solutions of ammonia of the same volumes but of different concentrations (2 to 50 mg.$L^{-1}$) with the same masses of each solid material maintained under stirring (160 rpm) for 120 min.

**Adsorption Kinetics of $NH_4^+$ on Developed Materials**

***Theoretical Approach***

The removal efficiency (R%) for ammonia ($NH_4^+$) and the equilibrium adsorption capacity ($q_t$) were calculated, respectively, by using the following equations:

Removal efficiency

$$R\% = \frac{(C_0 - C_t)}{C_0} \times 100 \quad (1)$$

The adsorption capacities of $NH_4^+$on different materials at any time (t) are expressed as $Q_t$ (mg. $g^{-1}$), which was calculated by Eq. (1):

$$q_t = \frac{(C_0 - C_t)\, V}{m} \quad (2)$$

where, $C_0$and Ct (mg $L^{-1}$) are the initial concentration and the concentration of $NH_4^+$ at time t, respectively. V (L) is the solution volume, and m(g) is the GEOM, Na-Mt and CAG mass.

***Adsorption Kinetics***

The kinetic data of $NH_4^+$ adsorption onto GEOM, Na-Mt, CAG, and CAC were described by the non-linear fitting of the pseudo-first-order, pseudo-second-order, and Elovich kinetic models (Wu et al., 2020), respectively.

**Adsorption Model**

Establishing the correct mathematical model is necessary to predict the adsorbent's adsorption behavior and optimize the adsorption process (Ren et al., 2021). The Langmuir and Freundlich isotherm models were introduced to evaluate the experimental equilibrium data by virtue of the method of non-linear analyses. The relevant equations are as follows:

***Langmuir Model***

$$q_e = \frac{q_{max} k_L C_e}{(1 + K_L C_e)} \quad (3)$$

The linearized form is:

$$\frac{C_e}{q_e} = \frac{1}{q_m k_1} + \frac{1}{q_m} C_e \quad (4)$$

***Freundlich Model***

$$q_e = k_F C_e^{1/n} \quad (5)$$

The linearized form is:

$$Lnq_e = Ln\, k_f + \frac{1}{n} Ln\, C_e \quad (6)$$

where, $k_F$=Freundlich isotherm constant (mg. $g^{-1}$), n=adsorption intensity; $C_e$=the equilibrium

concentration of adsorbate (mg.L$^{-1}$), and $q_e$ is the adsorption capacity at equilibrium on the adsorbent (mg.g$^{-1}$). $k_F$ and n are constants determined based on the experimental data (Khalil et al., 2018; Dada et al., 2012).

***Pseudo-First-Order Model***

The pseudo-first-order (PFO) kinetic model considers that the adsorption rate is directly positively related to the concentration of the adsorbate in the solution, and the resistance to mass transfer in the particles is the limiting factor. The equation is as follows (de Jesus Ruiz-Baltazar, 2018; Simonin, 2016):

$$q_t = q_e(e^{k_1 t}) \quad (7)$$

The linearized form is:

$$Ln\,(q_e - q_t) = Lnq_e - k_1 t \quad (8)$$

With $q_t$ represent the amount of adsorbed solute, $q_e$ its value at equilibrium, $k_1$ the pseudo-first order rate constant and t the time.

***Pseudo-Second-Order Model***

The (PSO) kinetic model considers that the adsorption rate is positively related to the square of the adsorbate concentration in the solution, and the adsorption mechanism mainly limits the adsorption rate. The equation is as follows (Shaban et al., 2017; de Jesus Ruiz-Baltazar, 2018):

$$q_t = k_2 q_e^2 t/(1 + k_2 q_e tq \quad (9)$$

The linearized form is:

$$t/q_t = t/q_e + 1/k_2 * q_e^2 \quad (10)$$

With $k_2$ is the pseudo-second order kinetic rate constant.

***Intraparticle Diffusion Model***

The intraparticle diffusion model **(IDM)** describes that substances undergo external and internal diffusion of substances in the adsorption process. It usually identifies the speed-limiting procedure in the whole adsorption course. The model is as follows (Dos Santos et al., 2014):

$$q_t = k_{id} t^{1/2} + C \quad (11)$$

Where, $k_{id}$ is the internal diffusion rate coefficient [mg/(g·min$^{1/2}$)], and C is a coefficient related to the thickness of the surface bounding layer of the adsorbent.

## Results and Discussion

**Characterization of Adsorbents**

***X-ray Diffraction (XRD)***

X-ray diffraction analysis of studied materials allows for identifying the crystallized mineral phases in the elaborated materials. In (Figure 2a, b) we notice a noticeable difference between the two diffractograms (Figure 2a, b) with a high percentage of montmorillonite in Na-Mt. The main peaks at (2θ=8.84°, 2θ=17.88° and 2θ=19.92°) present on the diffractograms are characteristic of the montmorillonite (Ait Hamoudi et al., 2014). On the other hand, the peak correlated at montmorillonite in GEOM is much less intense. This is caused by adding other constituents like activated carbon, cement and silica, causing a screen effect. In addition, traces of quartz are also present on these diffractograms, respectively at (2θ=25.20°, 2θ=26.67°, 2θ=27.56° and 2θ=37.79°) (Ait Hamoudi et al., 2014).

***Infrared Spectroscopy FTIR***

Infrared Spectroscopy spectra were recorded in a 4000-400 cm$^{-1}$ wavenumber range. The FTIR spectra of the montmorillonite (Figure 3) show the presence of absorption bands located in 3400 cm$^{-1}$ and 1630 cm$^{-1,}$ which characterize the state hydrated by Na-Mt. Bands located in 820 cm$^{-1}$ and 750 cm$^{-1}$ characterized bonds Al-O and Si-O responsible for the structure of the three-dimensional arrangement of the Na-Mt (Rodriguez-Iznaga et al., 2002). As shown in Figure 3, the FTIR of the geomaterial is more complex, while those of the composite contain bonds in common with cement, Na-Mt, silica, polymer, and activated carbon. FTIR shows the following functional groupings:

- Hydroxyls OH broad band at 3623 and 3449 cm $^{-1}$.
- AlMgOH and AlAlOH located at 817 and 921 cm $^{-1}$, respectively (Farmer, 1974; Ait Hamoudi et al., 2014)
- Al-OH at 913 and 793 cm $^{-1}$.
- Si-O-Al$^{iv}$ at 794 and 752 cm$^{-1}$.
- $H_2O$ in 1639 cm $^{-1}$.
- C=O at the region of 1860–1650 cm $^{-1}$ (stretching vibrations corresponding to carbonyl and carboxyl groups) (Moreno-Castilla et al., 2000).
- -$CH_2$ in 2918, 2988 cm $^{-1}$ (Ait Hamoudi et al., 2014)
- A broad tap in 3620 cm $^{1}$ allocated in bonds -OH in $H_2O$ (Ait Hamoudi et al., 2014).

***Surface Morphology by SEM (Scanning Electron Microscopy)***

The SEM method was used to observe the difference in morphology between Na-Mt and the prepared geomaterial GEOM. Corresponding results are shown in Figure 4. (a). Examining SEM images shows that the surface of a particle of the montmorillonite is in

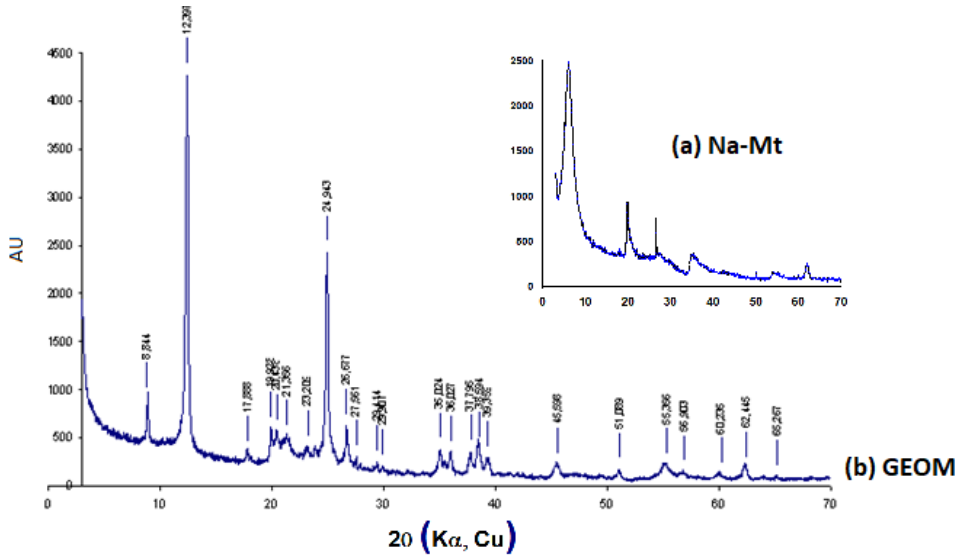


**Figure 2.** XRD-diffractogramms of (a) Na-Mt and (b) GEOM.

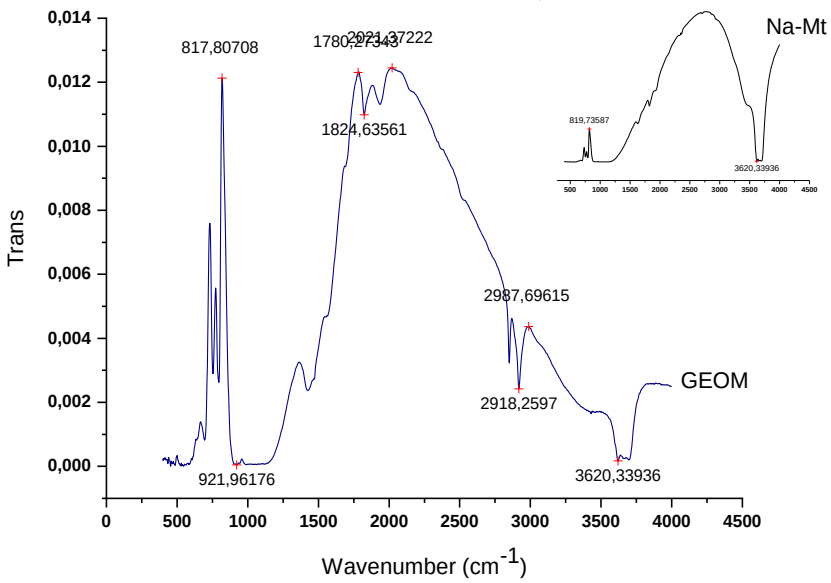


**Figure 3.** FTIR spectra of GEOM and Na-Mt.

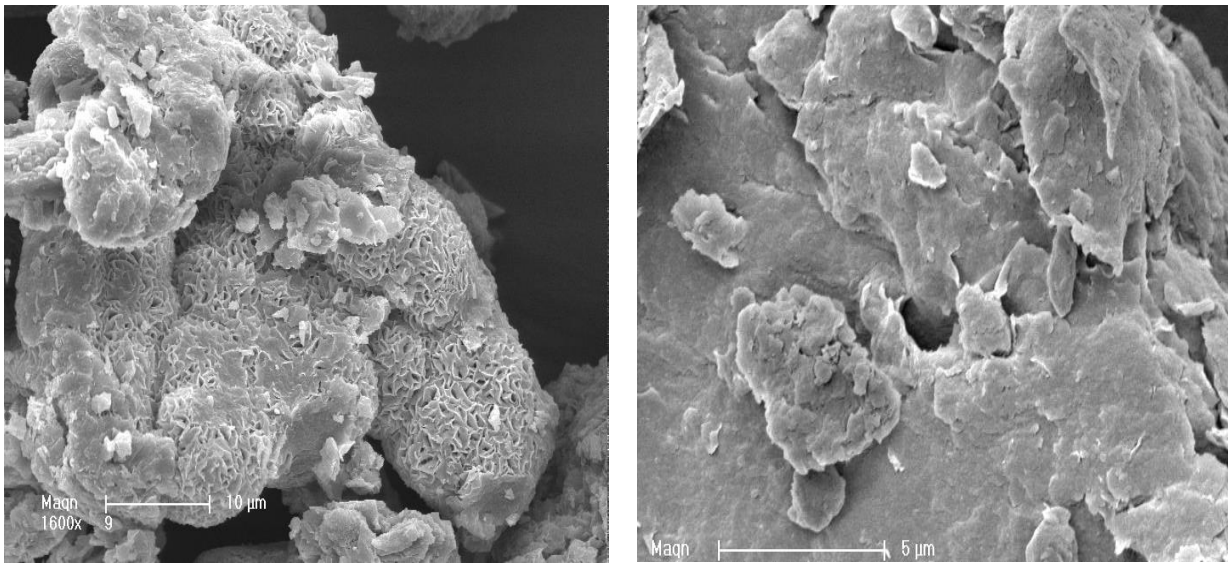


**Figure 4.** Scanning electron microscope 'SEM' images of Na-Mt (a) and GEOM (b).

the form of an aggregate of connected plans. Plans on the surface are orientated face against the face and seem very brought closer, with irregular forms that do not have defined borders. The bars of the montmorillonite have a regular morphology, ordered with particular forms. The size of each one is in the order of the micrometer but does not allow elementary bars to be differentiated. Moreover, they are piled up one on the other (crystals joined face to face) to constitute masses. This suggests a strong tendency to agglomerate this clay.

Furthermore, SEM images of GEOM in Figure 4 (b) indicate the heterogeneity of its structure. Indeed, we observe an assembly of several carbonaceous, silicate and aluminosilicate constituents. The presence of clay layers on the GEOM is very noticeable.

**Chemical Composition**

Table 1 lists the Na-Mt's and the geocomposite's chemical compositions. The corresponding results show the following phenomena:

- The compounds do not contain harmful metal elements such as lead and cadmium.
- The high percentage of carbon detected in the geocomposite is due to the presence of activated carbon, cement, and polymer.
- The analyzed materials are formed largely by alumino-silicate $SiO_2$ and $Al_2O_3$ (Konan, 2006).
- These results confirm the mineralogical study carried out by XRD.

**Ammonia Removal by Developed Materials: Adsorption Kinetics**

The study of adsorption kinetics is important for evaluating the efficiency of ionic ammonia removal by the adsorption process on the studied materials. This part was conducted to select the optimal contact time for isotherm experiments. We first conducted kinetic studies at pH 6.4 using Na-Mt, GEOM, CAC, and CAG sorbents. The plots of $q_e$ against $C_e$ for all elaborate adsorbents are reported in Figure 5.

**Table 1.** Chemical composition of studied adsorbents

| Element | Element % | Atomic % | Element % | Atomic % |
|---|---|---|---|---|
| | Na-Mt | | GEOM | |
| C | 8.18 | *12.51* | 64.99 | *74.26* |
| O | 56.16 | *64.50* | 23.75 | *20.37* |
| Na | 1.11 | *0.89* | 0.43 | *0.26* |
| Mg | 2.05 | *1.55* | 0.50 | *0.28* |
| Al | 7.51 | *5.11* | 2.50 | *1.27* |
| Si | 21.69 | *14.19* | 6.51 | *3.18* |
| K | 0.71 | *0.33* | 0.31 | *0.11* |
| Ca | 0.45 | *0.21* | 0.15* | *0.05** |
| Fe | 2.16 | *64.5* | 0.87 | *0.21* |
| Total | 100 | *100* | 100 | *100* |

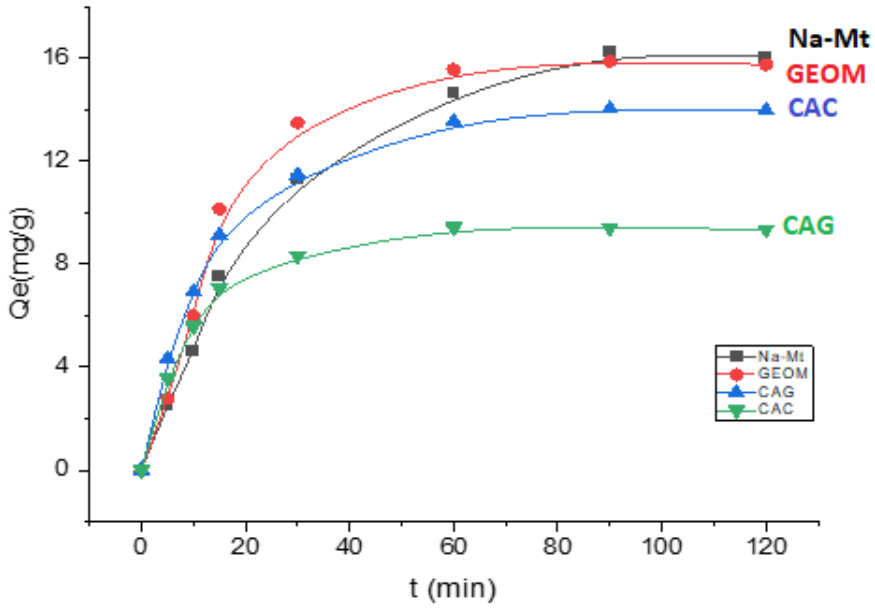


**Figure 5.** Adsorption kinetics of $NH_4^+$ on the studied adsorbents $C_0(NH_4^+)$ = 20 mg. $L^{-1}$, pH = 6.4; $m_0$ = 50 mg.

The four substrates show the same hyperbolic form characterized by fast and strong adsorption from the first minutes of contact (aqueous $NH_4^+$ adsorbate/adsorbent). For all elaborate materials, the shape of the curves in the first region of the graphs indicates that, as more exchange sites are occupied by $NH_4^+$, with the increase in contact time, it becomes more and more difficult for other $NH_4^+$ in solutions to find and replace exchangeable cations (Figure 6. a).

Adsorption rates are in the range of 81.05, 79.3, 67.7, and 46.7% for Na-Mt, GEOM, CAG, and CAC, respectively. Na-Mt has the best removal performance of $NH_4^+$ ions in an aqueous solution. Indeed, the purification of the raw clay by the elimination of its crystalline phases, such as quartz and calcite, and the homo-ionization with the monovalent $Na^+$ cation allowed the improvement of the CEC, which was confirmed by CEC analysis (Table 2) (the CEC increased from 65 for raw Mt to 92 meq/100g for purified homo-ionized Na-Mt).

These results are also consistent with the results obtained by (Maranon et al., 2006) related to the study of ammonium ion uptake from aqueous solutions using Romanian volcanic tuff. When the material is saturated with sodium ion $Na^{+}$, this promotes the exchange with $NH_4^+$ compared to other interfoliar cations (CEC of $NH_4^+$ at more affinity with sodium zeolite and Na-Mt, for example) (Sprynskyy et al., 2005; Praus et al., 2008; Calvo et al., 2009).

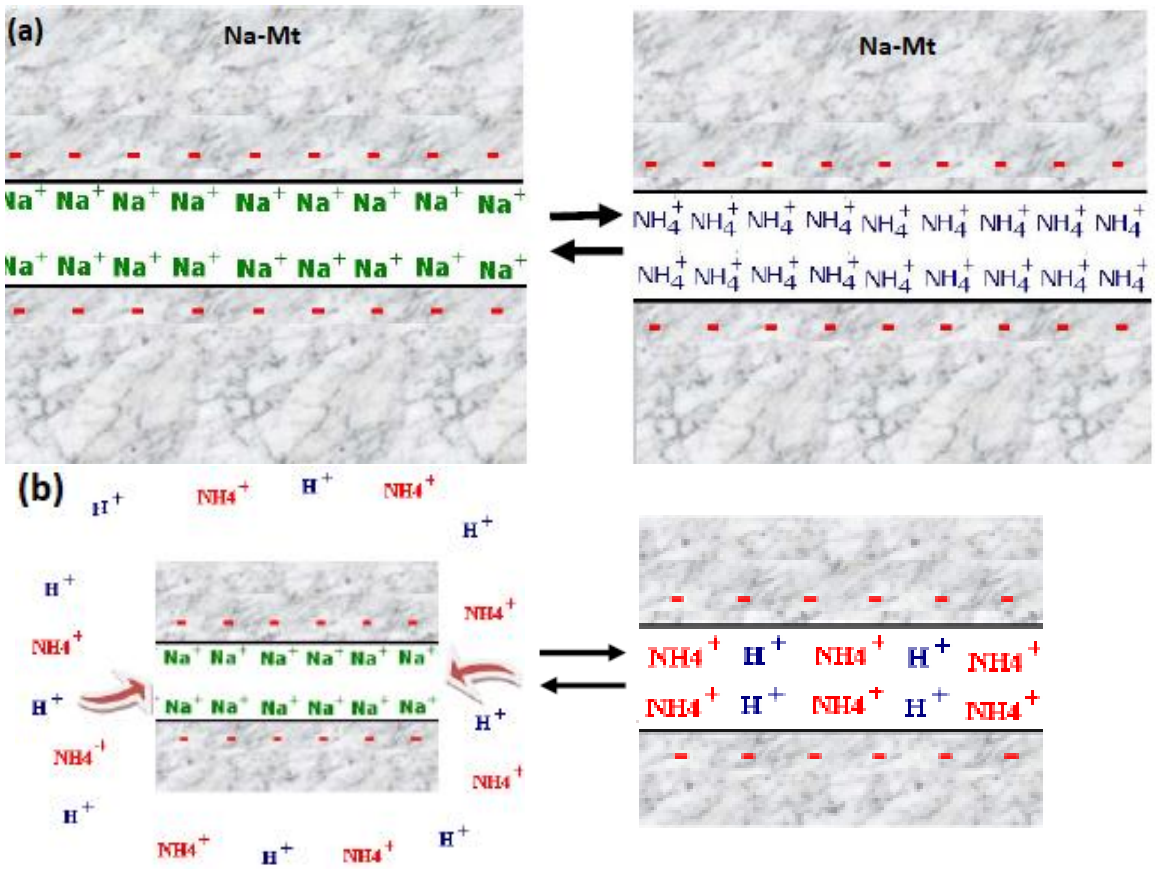


**Figure 6.** (a) Mechanism for removal of ammonium ions by cationic exchange in aluminosilicate material (Na-Mt and GEOM); (b) Illustration of competition of $NH_4^+$ and $H^+$ ions in the interfoliar space of aluminosilicate material.

**Table 2.** Physico-chemical parameters of the studied materials

| Parameter | Unite | Na-Mt | GEOM | CAG | CAC |
|---|---|---|---|---|---|
| Particle size | µm | $1,5 < \phi < 2,5$ | $0,5 < \phi < 1,5$ | $3 < \phi < 6$ | $1 < \phi < 3$ |
| Bulk density | $g.cm^{-3}$ | 2,22 | 2,05 | 0,71 | 0,80 |
| Apparent density | $g.cm^{-3}$ | 1,45 | 1,39 | 1,67 | 1,77 |
| Porosity | % | 34 | 32 | 57 | 54 |
| Specific surface area | $g.m^{-2}$ | 88,45 | 176,78 | 623 | 914 |
| Porous volume | $cm^3.g^{-1}$ | 0,23 | 0,111 | 0,80 | 0,68 |
| Microporous Volume, | $cm^3.g^{-1}$ | 0,098 | 0,078 | 0,37 | 0,38 |
| pH | - | 6,11 | 7,80 | 6, 71 | 6, 45 |
| CEC | Meq/100g | 92 | 71 | - | - |

Globally, the GEOM retention capacity seems to be slightly lower than bentonite but higher than CAG. This is due to its nature and composition. Earlier study (Seredych et al., 2008) on the retention of $NH_4^+$ by graphene and a geocomposite prepared by a mixture of (graphene/Na-Mt) showed a 50% increase in the retention capacity of $NH_4^+$ when Na-Mt is mixed with graphene. This result indicates that using the graphite/Na-Mt mixture improves the retention capabilities of $NH_4^+$ by the graphite.

In the second region of the graphs, we observed the presence of a semi-flat region, indicating a saturation condition (Ayawei et al., 2017). For the rest of our study, we fixed the contact time at 120 minutes.

**Effect of pH on Ammonia Removal**

In the adsorption process, the pH of the solution is an important parameter because of its role in the species solubilization, the surface of the adsorbent, and the rate of ionization of the adsorbate during the reaction. In this study, the effect of pH on ($NH_4^+$) removal has been studied in the range of pH between 3 and 11.

Figure 7 shows that ($NH_4^+$) retention increases when pH increases or approaches neutrality. It can be noted that the retention of ammonium by the four adsorbents is low when the pH range is below 6 (acidic pH). As the pH increases, the retention of ammonium ions increases. Thus, the optimal pH for Na-Mt is pH=6, corresponding to an elimination rate greater than 80%. Under these conditions, the optimal retention rate is 76 and 70% for GEOM and CAG, respectively.

In contrast, the optimal pH for CAC is in the neutral zone, with an $NH_4^+$ elimination rate of around 50%. So, for aluminosilicate adsorbent (Na-Mt and GEOM). The small amount of $NH_4^+$ removed by (Na-Mt and GEOM) in the acidic medium is linked to the strong competition between $H^+$ and $NH_4^+$ ions in the clay interfoliar system (Huang et al., 2010).

In a basic medium, the hydroxyl groups ($OH^-$) present in the solution could create bonds with the silicon atoms of incomplete tetrahedral. This leads to an increase in the density of negative charges of these sites. Also, a part of the $OH^-$ in solution will neutralize the population of $H^+$ protons present in the solution.

This state will have the consequence of increasing the number of negative charges on the surface, which will favor the binding of $NH_4^+$ by Na-Mt and geocomposite. Thus, the activation of the phenomenon of cation exchange by the release of $Na^+$ and retention of $NH_4^+$ cations in the absence of competition of $H^+$ ions (Figure 6. b). (Emerson et al., 1975) observed that for pH values below 7, ammonium exists mainly as $NH_4^+$, irrespective of temperature. On the other hand, at a strongly basic pH (pH > 9), the concentration of $NH_4^+$ ions in the solution decreases, which is accompanied by an increase in $NH_3$ (Emerson et al., 1975; Yusof et al., 2010). In such conditions, ammonia nitrogen may be present in ionized ($NH_4^+$) and non-ionized ($NH_3$) forms, the equilibrium of both species depending on pH and temperature values, according to the following equations:

$$NH_3 + H_2O \leftrightarrow NH_4^+ + OH^- \quad (12)$$

Acid $$NH_3 + H_3O^+ \leftrightarrow NH_4^+ + H_2O \quad (13)$$

Basic $$NH_4^+ + OH^- \leftrightarrow NH_3 + H_2O \quad (14)$$

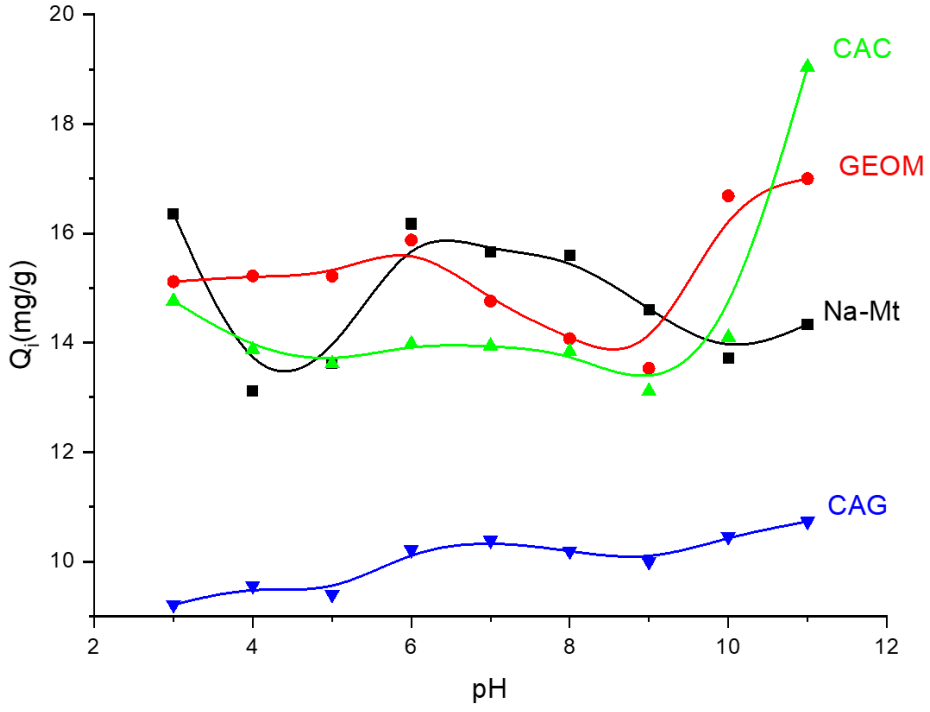


**Figure 7.** Influence of pH on the adsorption of $NH_4^+$ ion on the four studied substrates. $C_0$ ($NH_4^+$)=20 mg. $L^{-1}$, $m_0$=50 mg, T=20°C.

Therefore, the $NH_3$ molecular form is favored in a strongly basic medium (Eq. 14). In this case, the removal rate of ammonia is not related to adsorption by different adsorbents but rather to its chemical transformation.

Moreover, for carbonaceous materials, at pH < 6, the elimination of $NH_4^+$ by CAC and CAG solids is unfavorable, especially at low pH values. This phenomenon can be attributed to the disturbance of the $H^+$ or $H_3O^+$ protons in the vicinity of the active sites of activated carbon by electrostatic repulsion of the positive charges of the two cations (Zaini et al., 2009).

**Mechanism of Ammonium Removal by Different Prepared Materials**

***Adsorption Isotherms***

The adsorption data were fitted with Langmuir and Freundlich models to study the $NH_4^+$adsorption isotherms on the adsorbents. The fitting curves are presented in Figure 8 and 9, and the corresponding parameters are listed in Table 3. All calculations in this study were conducted using Microsoft Excel 2019. Depending on the correlation coefficient ($R^2$), all adsorption behaviors of $NH_4^+$ on the four studied adsorbents were fitted with the Langmuir and Freundlich equations, of which the Langmuir model was the best.

One of the essential characteristics of Langmuir isotherm could be expressed by a dimensionless constant called equilibrium parameter $R_L$, which is determined as follows (Eq. 15):

$$R_L = \frac{1}{(1 + k_1 C_0)} \quad (15)$$

Where, $k_1$ is a Langmuir constant and $C_0$ is the initial concentration. The value of $R_L$ is calculated using the above expression. The values of $R_L$ indicate the nature of the adsorption process (Lian, Guo, and Guo, 2009; Seliem et al., 2015).

| | |
|---|---|
| $R_L > 1$ | for unfavorable adsorption, |
| $R_L = 1$ | for linear adsorption, |
| $0 < R_L < 1$ | for favorable adsorption, |
| $R_L = 0$ | for irreversible adsorption. |

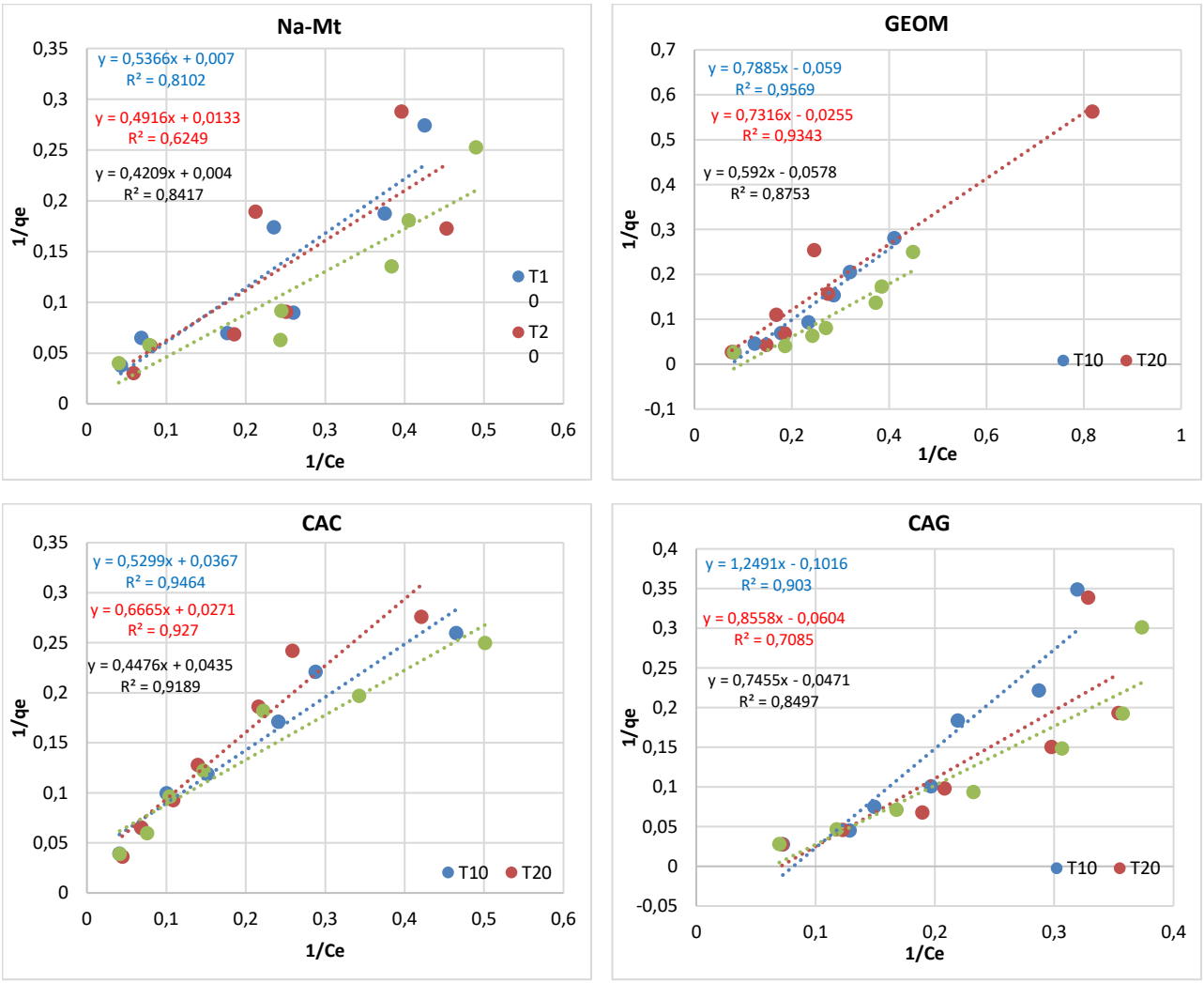


**Figure 8.** Langmuir isotherm plots for the uptake of $NH_4^+$ on the studied materials.

The maximum sorption capacities of $NH_4^+$ by the two used activated carbon (CAG and CAC) are less than those of Na-Mt and GEOM. Indeed, the maximum $NH_4^+$ adsorption capacity ($q_m$) of GEOM is 15.08 mg. $g^{-1}$, consistent with the experimental data (15.86 mg. $g^{-1}$, Table. 3). Conversely, and in the same conditions (T=20°C) for the other materials, the maximum $NH_4^+$ ($q_m$) are different from those obtained experimentally with $q_m$=75.18 mg. $g^{-1}$ for Na-Mt, $q_m$=37 mg. $g^{-1}$ for CAC and $q_m$=16.55 mg. $g^{-1}$ CAG (Table 3). This difference can be attributed to the predominance of the cation exchange phenomenon (Na-Mt and GEOM) compared to the adsorption phenomenon (CAG and CAC). Moreover, it can be seen that all adsorbent materials' best $NH_4^+$ removal efficiency is recorded at a higher temperature (at T=30°C) with 250, 17.3, 23, and 21 mg. $g^{-1}$ for Na-Mt, GOM, CAC, and CAG, respectively (Table 3).

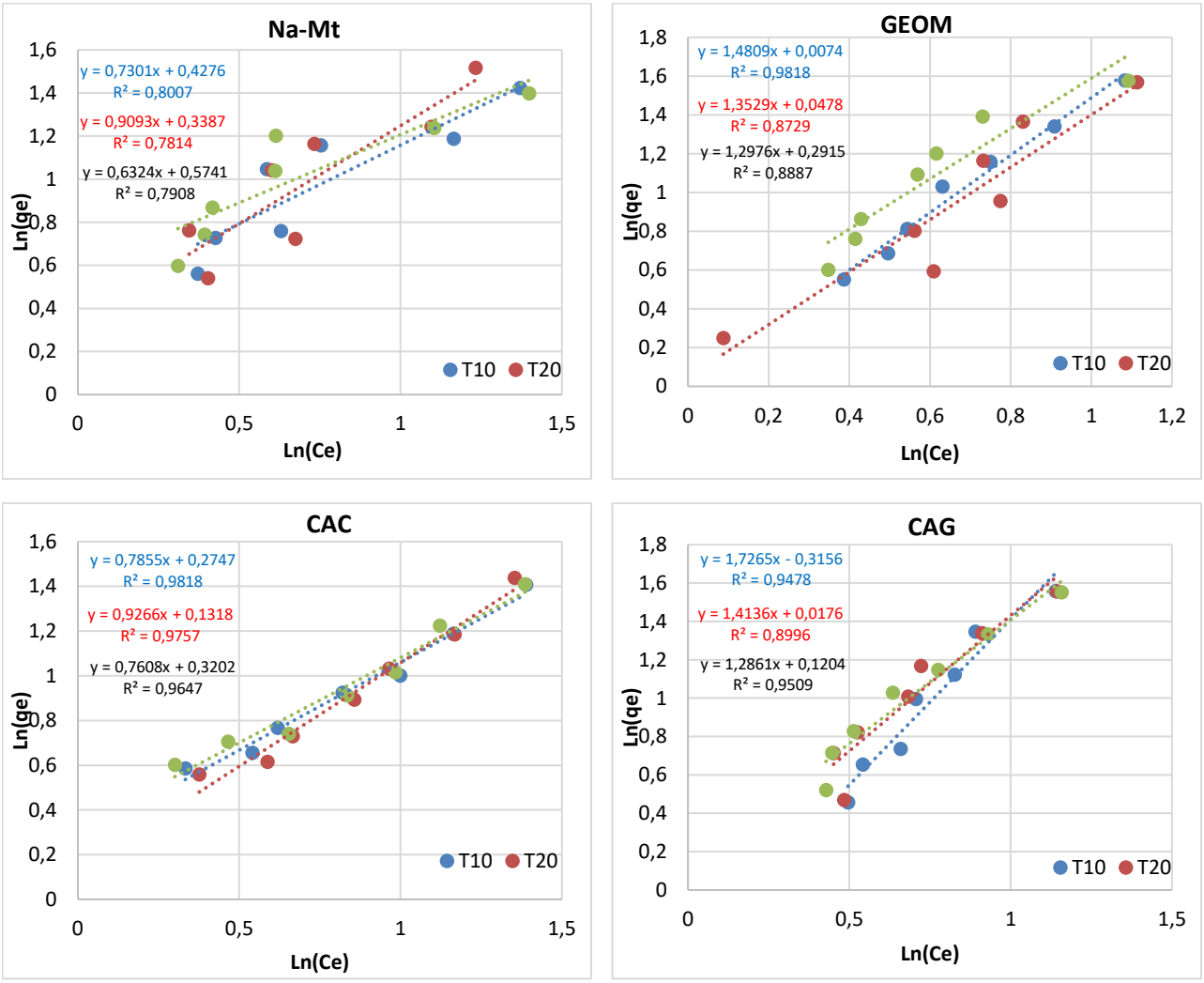


**Figure 9.** Freundlich isotherm plots for the uptake of $NH_4^+$ on the studied materials.

Table 3: Isotherm parameters for the adsorption of ($NH_4^+$) by studied adsorbents

| Adsorbent | T | Langmuir | | | | Freundlich | | | q(exp) (mgg$^{-1}$) |
|---|---|---|---|---|---|---|---|---|---|
| | | $K_L$ (L.mg$^{-1}$) | $q_m$ (mg. g$^{-1}$) | $R^2$ | $R_L$ | $k_F$ (L.g$^{-1}$) | $1/n_F$ | $R^2$ | |
| Na-Mt | 10°C | 0.013 | **142.85** | 0.8102 | 0,7937 | 2.676 | 0.7301 | 0.8007 | **16.21** |
| | 20°C | 0.027 | 75.18 | **0.6249** | 0,6494 | 2.181 | 0.9093 | **0.7814** | |
| | 30°C | 0.009 | **250** | 0.8417 | 0,8475 | 3.750 | 0.6324 | 0.7908 | |
| GEOM | 10°C | 0.075 | 17.00 | 0.9569 | 0,4000 | 2.068 | 1.7265 | 0.9478 | **15.86** |
| | 20°C | 0.313 | 15.08 | **0.9343** | 0,1377 | 1.041 | 1.4136 | **0.8996** | |
| | 30°C | 0.097 | 17.30 | 0.8753 | 0,3401 | 1.319 | 1.2861 | 0.9509 | |
| CAC | 10°C | 0.069 | 27.25 | 0.9464 | 0,4202 | 1.882 | 0.7855 | 0.9818 | **14.03** |
| | 20°C | 0.031 | 37.00 | **0.9270** | 0,6173 | 1.354 | 0.9266 | **0.9757** | |
| | 30°C | 0.058 | 23.00 | 0.9189 | 0,4630 | 2.090 | 0.7608 | 0.9647 | |
| CAG | 10°C | 0.081 | 09.84 | 0.9030 | 0,3817 | 1.017 | 1.4809 | 0.9818 | **09.40** |
| | 20°C | 0.070 | 16.55 | **0.7085** | 0,4167 | 1.116 | 1.3529 | **0.8729** | |
| | 30°C | 0.063 | 21.23 | 0.8497 | 0,4425 | 1.956 | 1.2976 | 0.8887 | |

These results suggested that ammonium adsorption onto these adsorbents was a mixture of monolayer adsorption and multilayer adsorption, resulting from the real heterogeneous nature of the surface sites involved in ammonia adsorption. The same results were reported by (Liu et al., 2010) in their study of ammonium adsorption by six agricultural residues. However, this would need to be confirmed by other thermodynamic studies in the future.

The Freundlich model is commonly utilized to explain adsorption for heterogeneous materials (Wasielewski et al., 2021). In our study, 1/n parameters were higher than 0.1 for all adsorbent materials, with 1.4, 0.9, 0.92, and 1.35 for GEOM, Na-Mt, CAC, and CAG, respectively (T=20°C). Corresponding values indicate favorable adsorption of $NH_4^+$ onto all elaborate materials. Several studies have also demonstrated that the adsorption process of $NH_4^+$ on various adsorbents was a better fit for the Freundlich model compared with other isotherm models, such as natural chabazite zeolite-rich tuff (Galamini et al., 2020), sepiolite (Balci, 2004), porous diatomite (AbuKhadra et al., 2020).

***Adsorption Kinetics***

Kinetics analysis is an important method for identifying the limiting-velocity procedure in the reaction process (Ren et al., 2021). To explore the kinetic process and adsorption mechanism of $NH_4^+$ on prepared adsorbents, a PFO, PSO as well as IPD kinetic models, were introduced to fit the test data. Figure 10a, b compares the linearized plots of the PFO and PSO. The values of the constants $k_1$ ($min^{-1}$), $k_2$ ($g.mg^{-1}.min^{-1}$), the correlation coefficients ($R^2$), the experimental and calculated adsorbed quantities $q_e$(exp) and $q_e$, as well as the extraction constant for the two models, are presented in Table 4.

As shown in Table 4, calculated qe for the pseudo-first-order are very small than $q_e$(exp) of studied materials. However, the calculated $q_e$ for all adsorbents closer to their experimental values: $q_e$=17.7, 15.75, 14.06, and 9.67 and $q_e$(exp)=16.21, 15.86, 14.03 and 9.40 for Na-Mt, GEOM, CAC and CAG, respectively. These results indicate that the $NH_4^+$ adsorption of prepared materials fitted well with the (PSO) kinetic

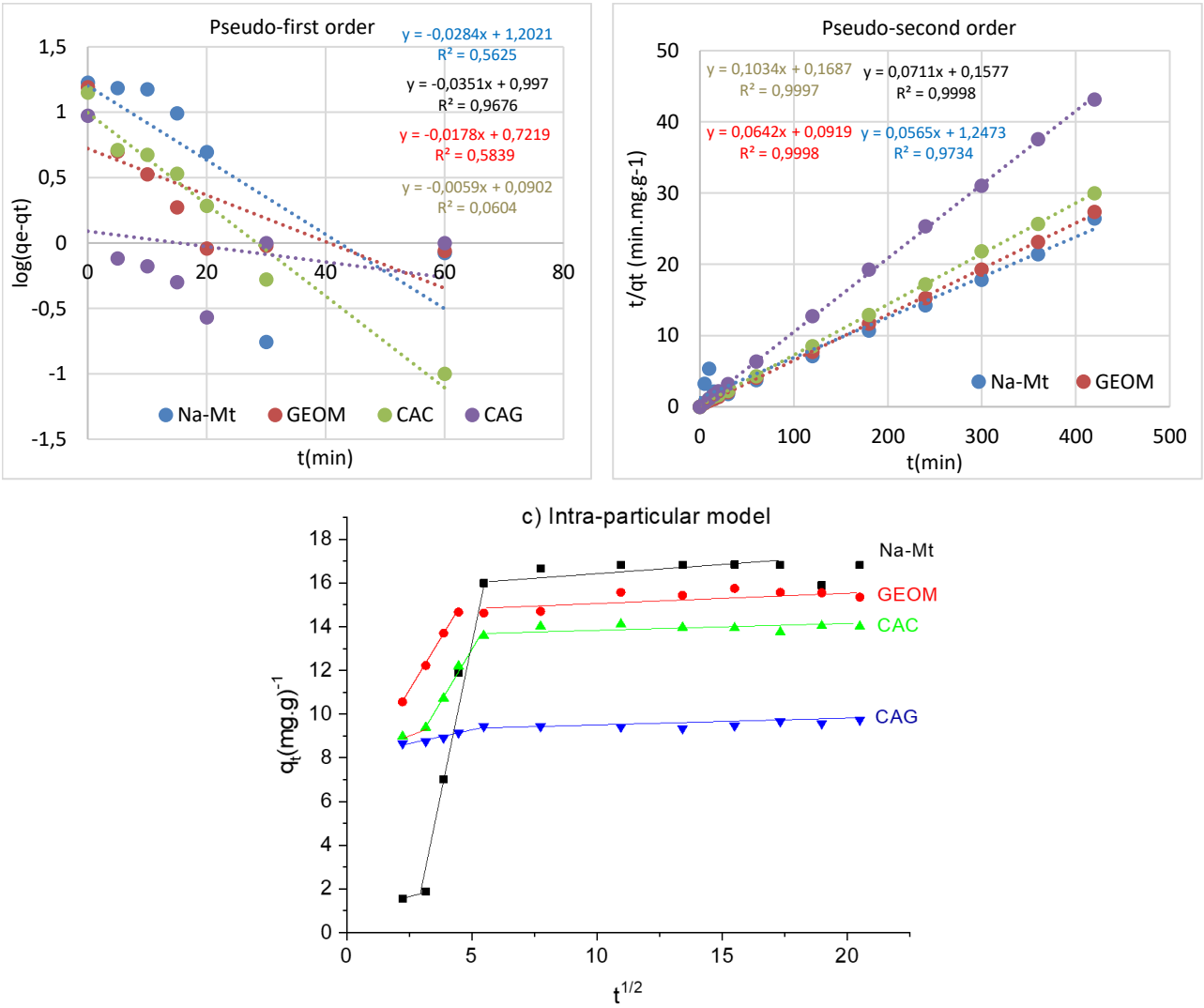


**Figure 10**. Linearized kinetics for $NH_4^+$ adsorption of all adsorbent materials: (a) Pseudo-first-order model, (b) Pseudo-second-order model and (c) intra-particular model.

model. The obtained ($q_e$) values confirm the evolution of the substrate efficiency obtained in the first experimental part of the kinetic study: $q_e$ (CAG) < $q_e$ (CAC) < $q_e$ (GEOM) < $q_e$ (Na-Mt). This result indicates that the adsorption of ammonium ($NH_4^+$) by aluminosilicates (Na-Mt and GEOM) is better represented by the (PSO) kinetic model than the adsorption by carbon materials (CAC and CAG). These results show also that the adsorption kinetics of $NH_4^+$ on various materials are consistent with the (PSO) kinetic model. Moreover, $R^2$ parameters for all prepared adsorbents are the highest for the (PSO) rate equation, which suggests that the prepared adsorbents adsorb $NH_4^+$ by the (PSO) mechanism (Kameda et al., 2021; Cheng, Zhu, and Xing, 2019).

In addition, the good adaptation of the experimental results and the linear regression to the (PSO) model suggest that the fixation of $NH_4^+$ on the studied materials is mainly due to chemisorption, which would imply forces and electron exchanges between the adsorbent and the adsorbate (Allaoui et al., 2021).Several authors have reported similar results. The (PSO) best predicts the $NH_4^+$ adsorption and other cations on the geopolymer, zeolite, sea shells, acid-aged biochar, ion exchange resins, and zeolite, respectively (Luukkonen et al., 2018; Wang, Li, Zhang, et al., 2020; Allaoui et al., 2021; Kameda et al., 2021; Al-Sheikh et al., 2021).

**Adsorption Mechanisms**

The intra-particle diffusion model was extensively studied to clarify the rate determining steps for studied materials further. This model can be used to elucidate the diffusion mechanism and investigate whether any intra-particle diffusion is the rate-limiting factor in the adsorption process. Figure 10 c shows the plots of $q_t$ against $t^{1/2}$ comprising two separate linear portions.

The linear regions of all the plots do not pass through the origin, which reveals that the adsorption of $NH_4^+$ on the studied materials was a complex process (Sun et al., 2018). The first step of a higher slope ($K_{id1}$) in all conditions, representing external diffusion of $NH_4^+$ on the adsorbent surfaces; the second step shows a decrease in the slope ($K_{id2}$) because of the increasing rate of adsorption reflected that the adsorption stage where intraparticle diffusion. However, the third region did not exist (horizontal line) because adsorption reached the equilibrium state (Wu et al., 2020). In addition, the adsorption rate followed the order of the first stage ($k_{p1}$) > second stage ($k_{p2}$) (Table 5). That was due to the decrement of active sites available for the adsorption, the low concentration of residual ammonium in the solution, and the thick boundary layer (Chen et al., 2016; Sun et al., 2018). This indicated that intra-particle diffusion was the rate-limiting step for the whole reaction.

**Influence of Water Composition on the Adsorption of $NH_4^+$ by the Prepared GEOM**

We examined the ability of GEOM to adsorb $NH_4^+$cations in the presence of salt water (filtered and sterilized seawater from CNRDPA's marine farm) and on a real aquaculture discharge to better understand the influence of the chemical nature of water on the adsorption of $NH_4^+$ by GEOM. The corresponding results (Figure 11) show that the yield of GEOM in seawater SW (high salinity; R=94.05%), or aquaculture effluent (complex composition; R=97.5%) and in ultrapure water (this study; ~80%), is always very important. This demonstrates that GEOM is an outstanding material that can be used to treat any water.

**Perspectives**

Low cost, high cation exchange capacity, surface reactivity due to silanol groups, and high affinity for cation metals are exceptional characteristics that make clay minerals attractive solids, with high demand for the preparation of various functional compounds.

**Table 4.** Kinetic parameters of the adsorption of ($NH_4^+$) by prepared adsorbents

| Adsorbent | Pseudo-first order | | | Pseudo-second order | | | q(exp) |
|---|---|---|---|---|---|---|---|
| | $K_1$ ($min^{-1}$) | $q_e$ (mg. $g^{-1}$) | $R^2$ | $K_2*10^{-4}$ g.(min.mg)$^{-1}$ | $q_e$ (mg. $g^{-1}$) | $R^2$ | (mg. $g^{-1}$) |
| Na-Mt | 0.0654 | 18.92 | 0.5625 | 39.81 | **17.7** | 0.9734 | **16.21** |
| GEOM | 0.0410 | 05.27 | 0.9676 | 3.78 | **15.57** | 0.9998 | **15.86** |
| CAC | 0.0800 | 09.93 | 0.5839 | 8 | **14.06** | 0.9998 | **14.03** |
| CAG | 0.0136 | 01.235 | 0.0640 | 18.03 | **09.67** | 0.9997 | **09.40** |

**Table 5.** Intra-particular model constants and correlation coefficients of $NH_4^+$ adsorption onto studied adsorbents

| Adsorbent | Intra-particular 1 | | | Intra-particular 2 | | |
|---|---|---|---|---|---|---|
| | $K_{id1}$ [mg/(g·$min^{1/2}$)] | C | $R^2$ | $K_{id2}$ [mg/(g·$min^{1/2}$)] | C | $R^2$ |
| Na-Mt | 6.33 | 12.55 | 0.997 | 0.002 | 16.80 | 0.706 |
| GEOM | 1.86 | 6.39 | 0.998 | 0.118 | 13.95 | 0.8677 |
| CAC | 1.874 | 5.03 | 0.987 | 0.003 | 13.78 | 1 |
| CAG | 0.249 | 8.02 | 0.957 | 0.021 | 9.243 | 0.654 |

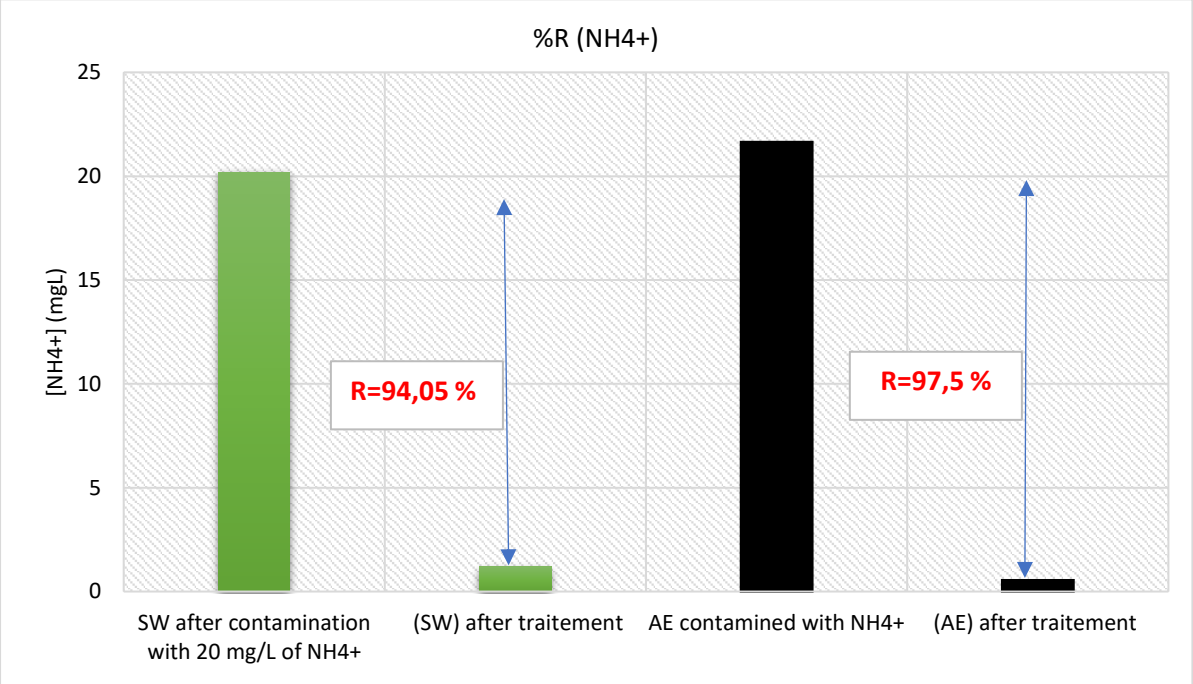


**Figure 11**. Influence of water composition on the adsorption of $NH_4^+$ by the elaborate GEOM.

The biofilter is a system consisting of filling material. Based on the promising findings presented in this paper, the GEOM can be used for stuffing biofilters as filter material. This preliminary study showed promising and encouraging results for treating contaminated water with ionic ammonia ($NH_4^+$) through local carbonated and aluminosilicate materials. To prove the application of these materials as filter materials in the biofiltration process, it is imperative to complete this study with several actions, including:

- adsorption study of nitrogen and carbon pollutants in dynamic conditions;
- GEOM granulation and its mechanical strength;
- possibility of combining adsorption methods with biological methods. Indeed, prepared GEOM is a very rough filter material that is favorable for the development of bacteria and will contribute to eliminating nitrogen pollutants (ammonium, nitrates, and nitrites).

## Conclusion

Characterization by SEM, XRD, FTIR and BET methods showed that GEOM sorbents are characterized by a mesoporous surface, a hydrophilic chemical surface, a specific surface relatively moderate and a high cation exchange capacity. Based on the results related to effects of contact time, initial ammonium concentration, pH, temperature, and coexisting cations on $NH_4^+$ removal, it can be concluded that using GEOM as an adsorbent material in ammonia elimination has been very successful. For all prepared materials, the neutrality zone was shown to be the best condition for removing ionized ammonia $NH_4^+$ for all prepared materials. The results showed that the (PSO) kinetic was more consistent with the adsorption of ammonia nitrogen. Langmuir and Freundlich's adsorption isotherm studies demonstrated that the mechanism of ammonia nitrogen removal was by electrostatic interactions. The proposed material can be readily used as filter material in the biofiltration process for aquaculture wastewater treatment.

## Ethical Statement

The authors declare that they did not use animals in their experiments.

## Funding Information

The authors declare they have no financial interests.

## Author Contribution

Belhouchet Nassima**:** Conceptualization, Writing - review and editing, data Curation, Formal Analysis, Investigation,

Hamdi Boualem: Methodology, performed of the experiments and Supervision

Bouras Omar: review and editing; Supervision

All authors reviewed the manuscript.

## Conflict of Interest

The authors declare that they have no known competing financial or non-financial, professional, or personal conflicts that could have appeared to influence the work reported in this paper.

## References


AbuKhadra, M. R., Eid, M. H., Allam, A. A., Ajarem, J. S., Almalki, A. M., & Salama, Y. (2020). Evaluation of different forms of Egyptian diatomite for the removal of ammonium ions from Lake Qarun: A realistic study to avoid eutrophication. *Environmental Pollution*, 266, 115277.

Ahmad, A. L., Chin, J. Y., Harun, M. H. Z., & Low, S. C. (2022). Environmental impacts and imperative technologies towards sustainable treatment of aquaculture wastewater: A review. *Journal of Water Process Engineering*, 46, 102553.

Ait Hamoudi, S., Hamdi, B., Brendlé, J., & Kessaissia, Z. (2014). Adsorption of lead by geomaterial matrix: Adsorption equilibrium and kinetics. *Separation Science and Technology*, 49, 1416-1426.

Allaoui, M., Berradi, M., Bensalah, J., Es-sahbany, H., Dagdag, O., & Ahmed, S. I. (2021). Study of the adsorption of nickel ions on the sea shells of Mehdia: Kinetic and thermodynamic study and mathematical modelling of experimental data. Materials Today: Proceedings, 45, 7494-7500.

Al-Sheikh, F., Moralejo, C., Pritzker, M., Anderson, W. A., & Elkamel, A. (2021). Batch adsorption study of ammonia removal from synthetic/real wastewater using ion exchange resins and zeolites. *Separation Science and Technology*, 56, 462-473.

Aminot, A., & Chaussepied, M. (1983). Manuel des analyses chimiques en milieu marin (No. 551.464 AMI). Brest: Centre national pour l'exploitation des océans.

Ayawei, N., Ebelegi, A. N., & Wankasi, D. (2017). Modeling and interpretation of adsorption isotherms. *Journal of Chemistry*, 2017, 3039817.

Balci, S. (2004). Nature of ammonium ion adsorption by sepiolite: Analysis of equilibrium data with several isotherms. *Water Research*, 38, 1129-1138.

Belhouchet, N., Inal, A., Nait-Mohand, H., Belkacem, Y., & Chenchouni, H. (2024). Assessment of pollutants in coastal waters, sediments, and biota of marine ecosystems in Algeria, North Africa. *Regional Studies in Marine Science*, 70, 103355.

Bernet, N., Delgenes, N., Akunna, J. C., Delgenès, J.-P., & Moletta, R. (2000). Combined anaerobic-aerobic SBR for the treatment of piggery wastewater. *Water Research*, 34, 611-619.

Blancheton, J. P., Attramadal, K. J. K., Michaud, L., Roque d'Orbcastel, E., & Vadstein, O. (2013). Insight into bacterial population in aquaculture systems and its implication. *Aquacultural Engineering*, 53, 30-39.

Boyd, C. E., D'Abramo, L. R., Glencross, B. D., Huyben, D. C., Juarez, L. M., Lockwood, G. S., ... Tomasso Jr, J. R. (2020). Achieving sustainable aquaculture: Historical and current perspectives and future needs and challenges. *Journal of the World Aquaculture Society*, 51, 578-633.

Calvo, B., Canoira, L., Morante, F., Martínez-Bedia, J. M., Vinagre, C., García-González, J.-E., ... Alcantara, R. (2009). Continuous elimination of $Pb^{2+}$, $Cu^{2+}$, $Zn^{2+}$, $H^{+}$ and $NH^{4+}$ from acidic waters by ionic exchange on natural zeolites. *Journal of Hazardous Materials*, 166, 619-627.

Chávez-Crooker, P., & Obreque-Contreras, J. (2010). Bioremediation of aquaculture wastes. *Current Opinion in Biotechnology*, 21, 313-317.

Chen, J., Yan, L. G., Yu, H. Q., Li, S., Qin, L. L., Liu, G. Q., ... & Du, B. (2016). Efficient removal of phosphate by facile prepared magnetic diatomite and illite clay from aqueous solution. *Chemical Engineering Journal*, 287, 162-172.

Cheng, C.-H., Ma, H.-L., Su, Y.-L., Deng, Y.-Q., Feng, J., Xie, J.-W., ... Guo, Z.-X. (2019). Ammonia toxicity in the mud crab (Scylla paramamosain): The mechanistic insight from physiology to transcriptome analysis. *Ecotoxicology and Environmental Safety*, 179, 9-16.

Cheng, H., Zhu, Q., & Xing, Z. (2019). Adsorption of ammonia nitrogen in low-temperature domestic wastewater by modification bentonite. *Journal of Cleaner Production*, 233, 720-730.

Cruz, H., Law, Y. Y., Guest, J. S., Rabaey, K., Batstone, D., Laycock, B., ... Pikaar, I. (2019). Mainstream ammonium recovery to advance sustainable urban wastewater management. *Environmental Science & Technology*, 53, 11066-11079.

Dada, A. O., Olalekan, A. P., Olatunya, A. M., & Dada, O. J. I. J. C. (2012). Langmuir, Freundlich, Temkin and Dubinin–Radushkevich isotherms studies of equilibrium sorption of $Zn^{2+}$ unto phosphoric acid modified rice husk. *IOSR Journal of Applied Chemistry*, 3, 38-45.

Dauda, A. B., Ajadi, A., Tola-Fabunmi, A. S., & Akinwole, A. O. (2019). Waste production in aquaculture: Sources, components, and managements in different culture systems. *Aquaculture and Fisheries*, 4, 81-88.

de Jesus Ruiz-Baltazar, A. (2018). Green composite based on silver nanoparticles supported on diatomaceous earth: Kinetic adsorption models and antibacterial effect. *Journal of Cluster Science*, 29, 509-519.

DeCoste, J. B., & Peterson, G. W. (2014). Metal–organic frameworks for air purification of toxic chemicals. *Chemical Reviews*, 114, 5695-5727.

Değermenci, N., & Yildiz, E. (2021). Ammonia stripping using a continuous flow jet loop reactor: mass transfer of ammonia and effect on stripping performance of influent ammonia concentration, hydraulic retention time, temperature, and air flow rate. *Environmental Science and Pollution Research*, 28(24), 31462-31469.

Dunegan, W. (2020). Quantifying the Water-Atmosphere Flux of Ammonia for the Estuaries of the Texas Coastal Bend. Doctoral dissertation, Texas A&M University-Corpus Christi.

Emerson, K., Russo, R. C., Lund, R. E., & Thurston, R. V. (1975). Aqueous ammonia equilibrium calculations: Effect of pH and temperature. *Journal of the Fisheries Board of Canada*, 32, 2379-2383.

Farmer, V. C. (1974). The Infrared Spectra of Minerals. *Mineralogical Society Monograph*, 4, 331-363.

Galamini, G., Ferretti, G., Medoro, V., Tescaro, N., Faccini, B., & Coltorti, M. (2020). Isotherms, kinetics, and thermodynamics of NH4+ adsorption in raw liquid manure by using natural chabazite zeolite-rich tuff. *Water*, 12, 2944.

Gephart, J. A., Golden, C. D., Asche, F., Belton, B., Brugere, C., Froehlich, H. E., ... Jones, R. C. (2020). Scenarios for global aquaculture and its role in human nutrition. *Reviews in Fisheries Science and Aquaculture*, 29, 122-138.

Hamdi, B., Houari, M., Ait Hamoudi, S., & Kessaïssia, Z. (2004). Adsorption of some volatile organic compounds on geomaterials. *Desalination*, 166, 449-455.

Hammer, H. S. (2020). Recirculating aquaculture systems (RAS) for zebrafish culture. In: The Zebrafish in Biomedical Research (pp. 337-356). Academic Press.

Han, B., Butterly, C., Zhang, W., He, J.-z., & Chen, D. (2021).

Adsorbent materials for ammonium and ammonia removal: A review. *Journal of Cleaner Production*, 283, 124611.

Haywood, G. P. (1983). Ammonia toxicity in teleost fishes: A review. *Can. Tech. Rep. Fish. Aquat. Sci*, 1177, 1-35.

Houari, M., Hamdi, B., Bouras, O., Bollinger, J.-C., & Baudu, M. (2014). Static sorption of phenol and 4-nitrophenol onto composite geomaterials based on montmorillonite, activated carbon and cement. *Chemical Engineering Journal*, 255, 506-512.

Houari, M., Hamdi, B., Brendle, J., Bouras, O., Bollinger, J. C., & Baudu, M. (2007). Dynamic sorption of ionizable organic compounds (IOCs) and xylene from water using geomaterial-modified montmorillonite. *Journal of Hazardous Materials*, 147, 738-745.

Huang, H., Xiao, X., Yan, B., & Yang, L. (2010). Ammonium removal from aqueous solutions by using natural Chinese (Chende) zeolite as adsorbent. *Journal of Hazardous Materials*, 175, 247-252.

Ip, Y. K., Chew, S. F., & Randall, D. J. (2001). Ammonia toxicity, tolerance, and excretion. *Fish Physiology*, 20, 109-148.

Jiang, W., Tian, X., Li, L., Dong, S., Zhao, K., Li, H., & Cai, Y. (2019). Temporal bacterial community succession during the start-up process of biofilters in a cold-freshwater recirculating aquaculture system. *Bioresource Technology*, 287, 121441.

John, E. M., Krishnapriya, K., & Sankar, T. V. (2020). Treatment of ammonia and nitrite in aquaculture wastewater by an assembled bacterial consortium. *Aquaculture*, 526, 735390.

Kameda, T., Kikuchi, H., Kitagawa, F., Kumagai, S., Saito, Y., Kondo, M., ... & Yoshioka, T. (2021). Ammonia adsorption by L-type zeolite and Prussian blue from aqueous and culture solutions. *Colloids and Surfaces A: Physicochemical and Engineering Aspects*, 622, 126595.

Khalaf. H, Bouras. O, Perrichon. V. (1997). Synthesis and characterization of Al-pillared and cationic surfactant modified Al-pillared Algerian bentonite, *Microporous Materials* 8-141-150.

Khalil, A., Sergeevich, N., & Borisova, V. (2018). Removal of ammonium from fish farms by biochar obtained from rice straw: Isotherm and kinetic studies for ammonium adsorption. *Adsorption Science & Technology*, 36, 1294-1309.

Konan, K. L. (2006). Interaction entre des matériaux argileux et un milieu basique riche en calcium [Interaction between clay materials and a calcium-rich basic environment]. Limoges.

Lee, J., Kim, I.-S., Emmanuel, A., & Koh, S.-C. (2019). Microbial valorization of solid wastes from a recirculating aquaculture system and the relevant microbial functions. *Aquacultural Engineering*, 87, 102016.

Lian, L., Guo, L., & Guo, C. (2009). Adsorption of Congo red from aqueous solutions onto Ca-bentonite. *Journal of Hazardous Materials*, 161, 126-131.

Liu, H., Dong, Y., Liu, Y., & Wang, H. (2010). Screening of novel low-cost adsorbents from agricultural residues to remove ammonia nitrogen from aqueous solution. *Journal of Hazardous Materials*, 178, 1132-1136.

Liu, N., Sun, Z., Zhang, H., Klausen, L. H., Moonhee, R., & Kang, S. (2023). Emerging high-ammonia-nitrogen wastewater remediation by biological treatment and photocatalysis techniques. *Science of the Total Environment*, 875, 162603.

Liu, W., Ke, H., Xie, J., Tan, H., Luo, G., Xu, B., & Abakari, G. (2020). Characterizing the water quality and microbial communities in different zones of a recirculating aquaculture system using biofloc biofilters. *Aquaculture*, 529, 735624.

Luukkonen, T., Věžníková, K., Tolonen, E.-T., Runtti, H., Yliniemi, J., Hu, T., ... Lassi, U. (2018). Removal of ammonium from municipal wastewater with powdered and granulated metakaolin geopolymer. *Environmental Technology*, 39, 414-423.

Maranon, E., Ulmanu, M., Fernandez, Y., Anger, I., & Castrillón, L. (2006). Removal of ammonium from aqueous solutions with volcanic tuff. *Journal of Hazardous Materials*, 137, 1402-1409.

Mavraganis, T., Constantina, C., Kolygas, M., Vidalis, K., & Nathanailides, C. (2020). Environmental issues of Aquaculture development. *Egyptian Journal of Aquatic Biology and Fisheries*, 24, 441-450.

Melouki, A., Terchi, S., Ouali, D., & Bounab, A. (2022). Preparation of new copolymer (polystyrene/TMSPM grafted on DDA-fractionated Algerian montmorillonite) hybrid organoclay by radical copolymerization: Structural study, thermal stability and hydrophobicity area. *Journal of Thermal Analysis and Calorimetry*, 147, 5637-5648.

Mook, W. T., Chakrabarti, M. H., Aroua, M. K., Khan, G. M. A., Ali, B. S., Islam, M. S., & Abu Hassan, M. A. (2012). Removal of total ammonia nitrogen (TAN), nitrate and total organic carbon (TOC) from aquaculture wastewater using electrochemical technology: A review. *Desalination*, 285, 1-13.

Moreno-Castilla, C., López-Ramón, M. V., & Carrasco-Marín, F. (2000). Changes in surface chemistry of activated carbons by wet oxidation. *Carbon*, 38, 1995-2001.

Nora'aini, A., Mohammad, A. W., Jusoh, A., Hasan, M. R., Ghazali, N., & Kamaruzaman, K. (2005). Treatment of aquaculture wastewater using ultra-low pressure asymmetric polyethersulfone (PES) membrane. *Desalination*, 185, 317-326.

Person-Le Ruyet, J., & Bœuf, G. (1998). L'azote ammoniacal, un toxique potentiel en élevage de poissons: Le cas du turbot. *Bulletin Français de la Pêche et de la Pisciculture*, 393-412.

Peterson, B. J., Bahr, M., & Kling, G. W. (1997). A tracer investigation of nitrogen cycling in a pristine tundra river. *Canadian Journal of Fisheries and Aquatic Sciences*, 54, 2361-2367.

Praus, P., Turicová, M., & Valásková, M. (2008). Study of silver adsorption on montmorillonite. *Journal of the Brazilian Chemical Society*, 19, 549-556.

Preena, P. G., Kumar, V. J. R., & Singh, I. S. B. (2021). Nitrification and denitrification in recirculating aquaculture systems: The processes and players. *Reviews in Aquaculture*, 13, 2053-2075.

Radu, G., & Racoviteanu, G. (2021, May). Removing ammonium from water intended for human consumption. A review of existing technologies. *IOP Conference Series: Earth and Environmental Science*, Vol. 664, No. 1, p. 012029). IOP Publishing.

Ren, Z., Jia, B., Zhang, G., Fu, X., Wang, Z., Wang, P., & Lv, L. (2021). Study on adsorption of ammonia nitrogen by iron-loaded activated carbon from low temperature wastewater. *Chemosphere*, 262, 127895.

Roalkvam, I., Drønen, K., Dahle, H., & Wergeland, H. I. (2020). Comparison of active biofilm carriers and commercially available inoculum for activation of biofilters in marine

recirculating aquaculture systems (RAS). *Aquaculture*, 514, 734480.

Rosenthal, H. (1993). Recirculation systems in aquaculture. In: Techniques for modern aquaculture, pp. 284-294.

Ruiz, P., Vidal, J. M., Sepúlveda, D., Torres, C., Villouta, G., Carrasco, C., ... Urrutia, H. (2020). Overview and future perspectives of nitrifying bacteria on biofilters for recirculating aquaculture systems. *Reviews in Aquaculture*, 12, 1478-1494.

Schreier, H. J., Mirzoyan, N., & Saito, K. (2010). Microbial diversity of biological filters in recirculating aquaculture systems. *Current Opinion in Biotechnology*, 21, 318-325.

Seliem, M. K., Mohamed, E. A., Selim, A. Q., Shahien, M. G., & Abukhadra, M. R. (2015). Synthesis of Na-A zeolites from natural and thermally activated Egyptian kaolinite: Characterization and competitive adsorption of copper ions from aqueous solutions. *International Journal of Bioassays*, 4, 4423-4430.

Seredych, M., Tamashausky, A. V., & Bandosz, T. J. (2008). Surface features of exfoliated graphite/bentonite composites and their importance for ammonia adsorption. *Carbon*, 46, 1241-1252.

Shaban, M., Abukhadra, M. R., Shahien, M. G., & Khan, A. A. P. (2017). Upgraded modified forms of bituminous coal for the removal of safranin-T dye from aqueous solution. *Environmental Science and Pollution Research*, 24, 18135-18151.

Simonin, J.-P. (2016). On the comparison of pseudo-first order and pseudo-second order rate laws in the modeling of adsorption kinetics. *Chemical Engineering Journal*, 300, 254-263.

Sprynskyy, M., Lebedynets, M., Terzyk, A. P., Kowalczyk, P., Namieśnik, J., & Buszewski, B. (2005). Ammonium sorption from aqueous solutions by the natural zeolite Transcarpathian clinoptilolite studied under dynamic conditions. *Journal of Colloid and Interface Science*, 284, 408-415.

Su, Z., Liu, T., Guo, J., & Zheng, M. (2023). Nitrite oxidation in wastewater treatment: Microbial adaptation and suppression challenges. *Environmental Science and Technology*, 57, 12557-12570.

Sun, J., Chen, Y., Yu, H., Yan, L., Du, B., & Pei, Z. (2018). Removal of $Cu^{2+}$, $Cd^{2+}$, and $Pb^{2+}$ from aqueous solutions by magnetic alginate microsphere based on $Fe_3O_4$/MgAl-layered double hydroxide. *Journal of Colloid and Interface Science*, 532, 474-484.

Suprihatin, S., Cahyaputri, B., Romli, M., & Yani, M. (2017). Use of biofilter as pre-treatment of polluted river water for drinking water supply. *Environmental Engineering Research*, 22, 203-209.

Tuyet, D. T. A., Hiep, L. M., Binh, H. T., Huyen, L. T., Tang, S.-L., Chiang, P.-W., & Hao, D. M. (2022). A multi-step nitrifying microbial enrichment to remove ammonia and nitrite in brackish aquaculture systems. *Biodegradation*, 33, 373-388.

Wang, X., Li, J., Chen, J., Cui, L., Li, W., Gao, X., & Liu, Z. (2020). Water quality criteria of total ammonia nitrogen (TAN) and un-ionized ammonia ($NH_3$-N) and their ecological risk in the Liao River, China. *Chemosphere*, 243, 125328.

Wang, Z., Li, J., Zhang, G., Zhi, Y., Yang, D., Lai, X., & Ren, T. (2020). Characterization of acid-aged biochar and its ammonium adsorption in an aqueous solution. *Materials*, 13, 2270.

Wasielewski, S., Rott, E., Minke, R. & Steinmetz, H. 2021. Application of Natural Clinoptilolite for Ammonium Removal from Sludge Water. *Molecules,* 26**,** 114.

Wu, Z., Sun, Z., Liu, P., Li, Q., Yang, R., & Yang, X. (2020). Competitive adsorption of naphthalene and phenanthrene on walnut shell based activated carbon and the verification via theoretical calculation. *RSC Advances*, 10, 10703-10714.

Xu, Y., Chen, Y., Ma, C., Qiao, W., Wang, J., Ling, L., ... (2022). Functionalization of activated carbon fiber mat with bimetallic active sites for NH3 and H2S adsorption at room temperature. *Separation and Purification Technology*, 303, 122335.

Yusof, A. M., Keat, L. K., Ibrahim, Z., Majid, Z. A., & Nizam, N. A. (2010). Kinetic and equilibrium studies of the removal of ammonium ions from aqueous solution by rice husk ash-synthesized zeolite Y and powdered and granulated forms of mordenite. *Journal of Hazardous Materials*, 174, 380-385.

Zaini, M. A. A., Okayama, R., & Machida, M. (2009). Adsorption of aqueous metal ions on cattle-manure-compost based activated carbons. *Journal of Hazardous Materials*, 170, 1119-1124.